의학박사 학위논문

한국인의 안구부속조직 점막기원 림프종에서 *Chlamydophila psittaci* 감염 여부와 독시사이클린 치료의 반응에 따른 전체 유전자 메틸화 양상의 비교 분석

2014년 2월

서울대학교 대학원

의학과 안과학 전공

이 민 정

의학박사 학위논문

한국인의 안구부속조직 점막기원 림프종에서 *Chlamydophila psittaci* 감염 여부와 독시사이클린 치료의 반응에 따른 전체 유전자 메틸화 양상의 비교 분석

2014년 2월

서울대학교 대학원

의학과 안과학 전공

이 민 정

Analysis of Genome-wide DNA Methylation Profile According to *Chlamydophila psittaci* Infection and the Response to Doxycycline Treatment in Ocular Adnexal MALT Lymphoma of Korean

February 2014

Department of Ophthalmology
Seoul National University College of Medicine
Min Joung Lee

ABSTRACT

Background and purpose: Lymphomas of the ocular adnexa are the most common malignant tumor arising from the ocular adnexa. In Korea, extranodal marginal zone B-cell lymphoma of mucosa-associated lymphoid tissue (MALT) accounts for a higher proportion than in western countries. *Chlamydophila psittaci* (*Cp*) is suggested to be a possible etiologic agent for ocular adnexal MALT lymphoma and *Cp*-eradicating treatment using doxycycline antibiotics has been attempted as a first-line targeted therapy in South Korea. Epigenetic alterations in association with aberrant promoter hypermethylation are also observed in MALT lymphomas, but genome-wide screening of DNA methylation profiles has not been performed. In this study, we compared genome-wide DNA methylation profiles according to *Cp* infection status and the response to doxycycline treatment in a Korean ocular adnexal MALT lymphoma patients.

Methods: Twelve ocular adnexal MALT lymphoma cases were classified into two groups (6 *Cp*-positive cases and 6 *Cp*-negative cases). Among the 12 cases, 8 were treated with doxycycline as a first-line therapy, and they were divided into 2 groups according to their response to the treatment (4 Doxy-responders and 4 Doxy-nonresponders). The differences in the DNA methylation states of 27,578 methylation sites in 14,000 genes were evaluated using Illumina bead assay technology. We also validated the top-ranking differentially methylated genes (DMGs) by bisulfite direct sequencing or pyrosequencing.

Results: The Infinium Methylation chip assay revealed 180 DMGs in the *Cp*-

positive group (74 hypermethylated genes and 106 hypomethylated genes) compared to the *Cp*-negative group. Among the 180 DMGs, *DUSP22*, which had 2 significantly hypomethylated loci, was validated, and the correlation was significant for one CpG site (Spearman coefficient = 0.6478, $p = 0.0262$). With regard to the response to doxycycline treatment, a total of 778 DMGs were revealed (389 hypermethylated genes and 336 hypomethylated genes in the Doxy-responder group). In a subsequent replication study for representative hypomethylated (*IRAK1*) and hypermethylated (*CXCL6*) genes, the correlation between the bead chip analysis and pyrosequencing was significant (Spearman coefficient = 0.8961 and 0.7619, respectively, $p < 0.05$).

Conclusions: Ocular adnexal MALT lymphoma showed distinct methylation patterns according to *Cp* infection and the response to doxycycline treatment in this genome-wide methylation study. Among the candidate genes, *DUSP22* has a methylation status that was likely attributable to *Cp* infection. Our data also suggest that the methylation statuses of *IRAK1* and *CXCL6* may reflect the response to doxycycline treatment.

Keywords: Ocular adnexa; mucosa-associated lymphoid tissue lymphoma; methylation; *Chlamydophila psittaci*; doxycycline; *DUSP22*; *IRAK1*; *CXCL6*

Student number: 2008-31013

CONTENTS

List of Tables

List of Figures

INTRODUCTION

Lymphomas of the ocular adnexa account for approximately 8% of extranodal lymphomas and are the most common malignant tumor arising from the ocular adnexa (1, 2). The incidence has risen steadily between 1975 and 2001, with an annual increase of 6.3%, and some geographical differences in epidemiology have been reported (3, 4). In Korea, extranodal marginal zone B-cell lymphoma of mucosa-associated lymphoid tissue (MALT) accounts for a higher proportion (80-90 %) of all ocular adnexal lymphomas than in western countries (35-70%) (5-7). In addition, a younger age of onset, predominance of conjunctival involvement, earlier stage of diagnosis, and better prognosis are characteristic findings in Korean patients with ocular adnexal lymphoma (5). These geographically distinctive epidemiologic patterns suggest environmental and genetic factors, including microbiologic infection (3, 4, 8).

Among several microbiological agents, *Chlamydophila psittaci* (*Cp*) is suggested to be a possible etiologic agent. In 2004, Ferreri et al reported that *Cp* DNA was detected in 80% of ocular adnexal MALT lymphoma patients by targeted polymerase chain reaction (PCR) (9). However, subsequent studies revealed that the prevalence of *Cp* infection in ocular adnexal MALT lymphoma cases varied among countries (4, 10, 11). With respect to South Korea, a relatively higher prevalence of *Cp* –positivity (75-77%) has been repeatedly reported (12, 13). In addition, *Cp*-eradicating

treatment using doxycycline antibiotics has been attempted as a first-line targeted therapy in South Korea (4, 13, 14).

On the other hand, several genetic alterations have been reported in ocular adnexal MALT lymphomas (15). The most common are the translocations t(11;18)(q21;q21), t(14;18)(q32;q21), and t(1;14)(p22;q32), trisomy 3 and trisomy 18. Epigenetic alterations in association with aberrant promoter hypermethylation are also observed in MALT lymphomas. With regard to gastric MALT lymphoma, several studies have demonstrated that *Helicobacter pylori* (*Hp*) infection is associated with gene promoter hypermethylation or hypomethylation with specific methylation profiles (16, 17).

Recently, Choung et al (13) also reported the methylation profile of 9 tumor suppressor genes and reported that aberrant promoter methylation is a frequent event in ocular adnexal MALT lymphomas. However, genome-wide screening of DNA methylation profiles associated with ocular adnexa MALT lymphoma has not been performed. In the present study, we evaluated genome-wide DNA methylation profiles associated with *Cp*-infection and the response to doxycycline treatment.

MATERIALS AND METHODS

Patients

Twelve tissue samples were collected from patients who had undergone an incisional biopsy operation and had been histologically confirmed as a MALT lymphoma at Seoul National University Hospital, Seoul National University Bundang Hospital, and Seoul National University Boramae Hospital between 2011 and 2012. In the operating room, the tumor sample was immediately divided into 2 pieces; one piece of tissue was sent to the pathologist for histologic examinations, and the other piece was stored as fresh frozen status at -80℃ refrigerator. The histopathologic diagnosis of the sample was confirmed by a hematopathologist.

A staging workup was carried out based on a physical examination, complete ophthalmologic examination, chest radiograph, magnetic resonance imaging (MRI) of the orbit, computed tomography (CT) of the chest and abdomen, and bone marrow aspiration and biopsy. All patients were staged according to the American Joint Committee on Cancer classification (18).

All samples were examined for *Cp*-positivity and divided into two groups (6 *Cp*-positive samples and 6 *Cp*-negative samples) (Figure 1). Among the 12 patients, 8 patients were treated with doxycycline (100 mg twice a day for 3 weeks, 2 cycles) as a single, first-line treatment; they were followed for more than 6 months, and they were divided into two groups according to their treatment responses (4 Doxy-responders and 4 Doxy-nonresponders).

Doxycycline was given orally at a dose of 100 mg twice a day for 3 weeks, followed by 3 weeks of no doxycycline treatment, and then the treatment was repeated for an additional 3 weeks. The objective lymphoma response to the therapy was evaluated in all patients 9 weeks after the first-dose, then every 3 months for 2 years, and every 6 months thereafter by biomicroscopic examination or orbital imaging study (computed tomography or magnetic resonance image) by experienced oculoplasty specialists. The response was assessed using modified international workshop criteria (19). Complete remission (CR) was defined as the complete disappearance of all detectable ophthalmic and radiographic evidence of disease and eye-related symptoms, if they were present before therapy. Partial remission (PR) was defined as a 50% or more decrease in the sum of the product of the greatest diameters. Stable disease (SD) was defined as the regression of any measurable lesion by less than 50% or no change in the sizes of the measurable lesions. Progressive disease (PD) was defined by the development of any new lesion or by a 50% or more increase from the smallest sum of the product of the greatest diameters. The patient demographic and clinical data are shown in Table 1. The study was approved by the Committee on Human Research of the Seoul National University Hospital (IRB No. H-1012-086-344) and informed consent was obtained from all patients enrolled.

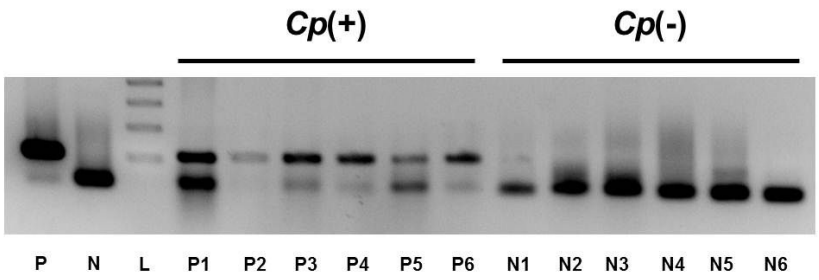

Figure 1. Amplification of *Chlamydophila psittaci* DNA using PCR. Six cases of 12 ocular adnexal MALT lymphoma showed positive bands and defined as *Cp*-positive samples, and the others were grouped as *Cp*-negative group. P, positive control for C. psittaci; N, negative control; L, size marker (100-bp DNA ladder).

Table 1. Clinical characteristics of the study subjects

Case No.	Age /Sex	Laterality	Tumor location (T stage*)	*Cp*	Initial treatment	Response to treatment†	Doxy Responder vs Non-responder	Follow-up-period (month)
P1	64/F	bilateral	Lacrimal gland (2b)	+	Doxycycline	CR	Responder	13
P2	39/F	unilateral	Conjunctiva (1b)	+	Doxycycline	CR	Responder	24
P3	43/M	unilateral	Orbit (2c)	+	Doxycycline	SD	Nonresponder	17
P4	51/M	bilateral	Conjunctiva (1b)	+	Doxycycline	PD	Nonresponder	36
P5	53/F	unilateral	Conjunctiva and orbit (2a)	+	Doxycycline	SD	Nonresponder	20
P6	29/F	bilateral	Conjunctiva (1b)	+	Doxycycline	-		4
N1	29/F	unilateral	Conjunctiva (1b)	-	Doxycycline	CR	Responder	34
N2	49/M	bilateral	Orbit (2c)	-	Doxycycline	SD	Nonresponder	15
N3	79/F	unilateral	Conjunctiva (1b)	-	Doxycycline	PR	Responder	15
N4	48/M	unilateral	Orbit and eyelid (3)	-	Radiation	CR	-	4
N5	68/F	bilateral	Orbit (2c)	-	-	-	-	-
N6	30/F	bilateral	Conjunctiva (1b)	-	Doxycycline	-	-	-

* American Joint Committee on Cancer staging (18)

† The response to the therapy was assessed 9 weeks after the first-dose, then every 3 months for 2 years, and then every 6 months afterward, using modified international workshop criteria (19)

Cp, *Chlamydophila psittaci*;, CR, complete response; PD, progressive disease; PR, partial response; SD, stable disease.

Detection of *Chlamydophila* DNA

Chlamydophila DNA was generously provided by Dr. Seung-Joon Lee of Kangwon National University, Korea. The DNA was amplified by PCR and cloned using the TOPO TA cloning kit (Invitrogen, Carlsbad, CA) according to the manufacturer's instructions. For verification, the cloned DNA was sequenced in both directions with Big Dye terminator (Applied Biosystems, Foster City, CA) and analyzed using an ABI 3730XL DNA analyzer (Applied Biosystems, Foster City, CA). For each extracted DNA sample, touchdown enzyme time-release PCR (TETR-PCR) for *Cp* was performed as described previously, but with some modification of the annealing temperature. Ta-CLONED *Chlamydophila* DNA was used as a positive control. The annealing temperature was 54°C. The amplified DNA fragments were electrophoresed on 2 % agarose gels and they were visualized after staining with ethidium bromide. To exclude the possibility of contamination of the extracted DNA, the PCR products positive for *Cp* DNA were sequenced.

DNA extraction and quality control

The genomic DNA was isolated using a QIAamp DNA mini kit (Qiagen, Hilden, Germany) according to the manufacturer's instructions. The average 260/280 ratio was 1.85. The quality of the DNA samples was checked using a NanoDrop® ND-1000 UV-Vis Spectrophotometer (Thermo Fisher Scientific, Waltham, MA, USA). Then, the samples were electrophoresed on agarose

gels, and the samples with intact genomic DNA, no smearing on the agarose gel, were selected for further experiments. The intact genomic DNA was diluted to 50 ng/$\mu\ell$, and the quantity of the DNA was determined using a PicoGreen dsDNA quantification kit (Invitrogen, Carlsbad, CA, USA).

Methylation profile

A genome-wide methylation profiling of 27,578 methylation sites in 14,000 genes was conducted by an Infinium Methylation Assay that combined the Illumina Infinium Whole Genome Genotyping (WGG) assay and BeadChip technology. The study included almost 13,000 genes in the NCBI CCDS (http://www.ncbi.nlm.nih.gov/CCDS) database (Genome Build 36), 144 markers of methylation hotspots in cancer genes, 982 markers of cancer-related targets, and 110 miRNA promoters. One random sample from the 12 samples was hybridized to different chips (technical replicate). We obtained high reproducibility in the technical replicates ($r^2 \geq 0.98$).

Data analysis

For measuring methylation, we used the Illumina Bead-Studio software to generate the level of methylation (ß) value for each locus from the intensity of methylated and unmethylated probes. The background normalization was conducted using the negative control signals from each well. Average normalization was performed to minimize the scanner-to-scanner variation;

the average intensity values of the first color channel for all the wells in each chip were used to calculate the mean value, which was scaled to 1. The ß was calculated as (intensity of methylated probe)/(intensity of methylated probe + intensity of unmethylated probe). Hence, ß ranged between 0 (least methylated) and 1 (most methylated) and was proportional to the degree of methylated state of any particular loci. The Infinium Methylation Chip data were analyzed with ArrayAssist software. To identify differentially methylated genes (DMGs) between the *Cp*-positive and *Cp*-negative samples or Doxy-responder and Doxy-nonresponder samples, we applied two significance criteria: (1) the *p*-value calculated using the Student t test and corrected for multiple testing with the Benjamini-Hochberg adjustment, and (2) the difference in mean ß-values (delta mean). The genes were defined as DMGs if their t-test p-values were < 0.05 and the |delta mean| (the absolute values of the delta mean) between the two groups were > 0.06. The resulting differential methylation profiles were analyzed with DAVID bioinformatics resources for the Gene Set Enrichment Analysis (GSEA). A hierarchical clustering analysis was based on the Euclidean distance matrix, and the complete linkage method was performed with an R package. The color scale of the heat map represents densely methylated loci (red) to sparsely methylated loci (green).

Bisulfite direct sequencing

The targeted fragment was amplified from bisulfite-treated DNA, cloned, and sequenced to obtain an accurate map of the distribution of CpG methylation. The PCR products were then cloned into the pEasy-T1 vector (Transgene, China), and ten colonies were randomly chosen and sequenced.

Pyrosequencing

Sodium bisulfite modification of the genomic DNA was performed. The primers were designed using the PSQ Assay Design program v.1.0.6 (Qiagen, Hilden, Germany), and the sequences are presented in Table 2. The pyrosequencing was conducted using PyroMark Gold Q96 Reagents (Qiagen, Hilden, Germany), and the PCR was conducted using Accupower HOT start PCR Premix (Bioneer, Daejeon, Korea). The pyrosequencing data were analyzed by Pyro Q-CpG V.1.0.9 analysis software (Qiagen, Hilden, Germany).

Table 2. Primer sequences for bisulfite sequencing or pyrosequencing

Genes	Method	Sequences	Tm (°C)	Product size (bp)
DUSP22 **(1st site)**	bisulfite sequencing	(F) 5′-GGGGAGTTTTTAGAGATTAGGTTTTT (R) 5′-AATCTCCAAATCCCCCTTTAAC	71	131
DUSP22 **(2nd site)**	bisulfite sequencing	(F) 5′- GTATAGAAAGTTTTGTTTTTTA (R) 5′- TATTCATCCCATTCCCCATAATA	81	226
IRAK1	pyrosequencing	(F) 5′- TTAAATGAGGGTTGGGGTAGTAGTAA (R) 5′- ACAACAACCTTAAACCATTCAATCTC	69	109
CXCL6	pyrosequencing	(F) 5′- GGTTATTGGAGAGGAGGAGTATTT (R) 5′- CAACAAAATCTCATCCCCTAAACTTA	68	95

Tm, annealing temperature

RESULTS

Differential Methylation According to Chlamydophila psittaci Infection

To investigate whether ocular adnexal MALT lymphomas have differential methylation patterns with respect to *Cp* infection status, a whole-genome methylation array analysis was carried out by using the Illumina Infinium Human Methylation 27 Bead Chip. A similar bimodal mean ß-value distribution was observed for both the *Cp*-positive and *Cp*-negative samples (Figure 2). When we compared all 27,578 loci, there was a total of 184 CpG sites that were differentially methylated at | delta mean | ≥ 0.06 and p-value < 0.05. Four pairs of loci corresponded to the same gene, 180 genes were considered to be differentially methylated. The *Cp*-positive samples showed hypermethylation in 75 of the CpG sites (40.8 %, 74 genes) and hypomethylation in 109 of the CpG sites (59.2 %, 106 genes). To assess the ability of the 184 differentially methylated loci to distinguish the *Cp*-positive group from the *Cp*-negative group, the methylation patterns of the sites were hierarchically clustered by measuring the Euclidian distance between the methylation levels across the loci (Figure 3). The samples were significantly segregated according to *Cp* status.

The results of the gene set analyses using PANTHER are shown in Table 3. The most significant annotation clusters of enriched gene sets (p<0.05) were inferred from functional annotation analysis with DMGs

according to their methylation statuses. The DMGs were enriched the most in genes for biologic processes related to immunity and defense (p=8.69E-07), followed by signal transduction (p=0.001) and lipid, fatty acid, and steroid metabolism (p=0.01). Regarding molecular function, DMGs were related to receptor (p=5.75E-08), ion channel (p=9.35E-05), and extracellular matrix (p=0.008).

We subsequently performed bisulfite direct sequencing for *DUSP22* (dual specificity protein phosphatase 22) which showed the most differentially methylated loci at two sites. *DUSP22* also belongs to the gene sets of immunity and defense and signal transduction. The primers and PCR conditions are described in Table 2. The methylation state of one CpG site showed a significant correlation with that of the Infinium methylation chip assay (Spearman coefficient=0.6478, p=0.0262); however, the other CpG site failed to replicate the result of the methylation array (Figure 4).

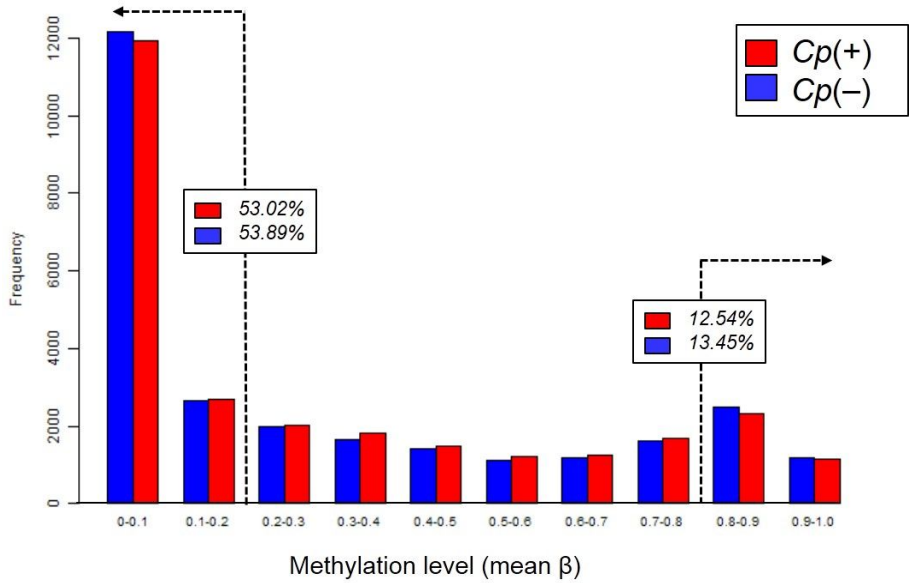

Figure 2. Distribution of the mean β-values of CpG sites in 6 *Cp*-positive and 6 *Cp*-negative ocular adnexal MALT lymphomas. The *Cp*-positive and *Cp*-negative groups showed similar bimodal distribution of methylation levels.

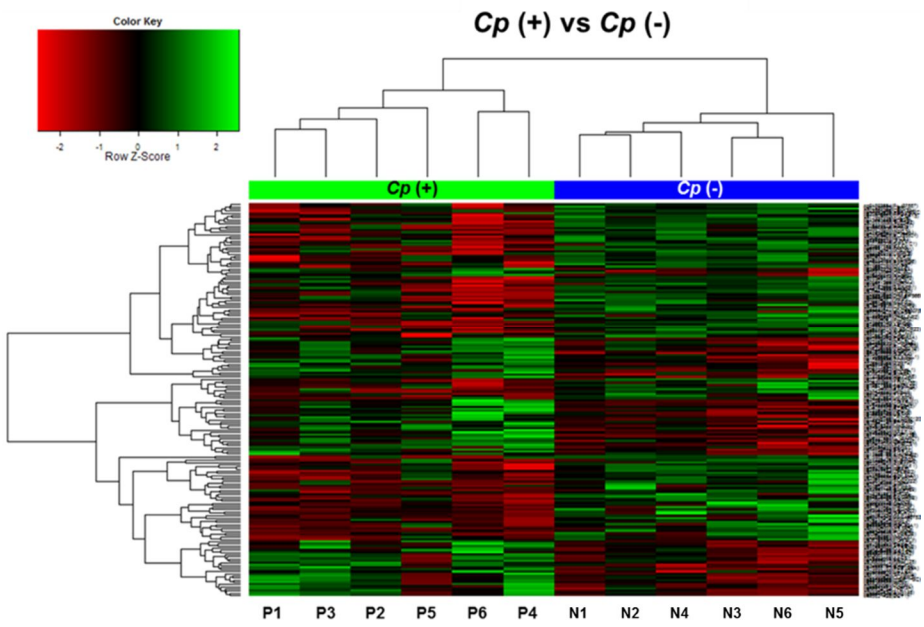

Figure 3. Hierarchical clustering analysis based on the DNA methylation data obtained from 6 *Cp*-positive and 6 *Cp*-negative ocular adnexal MALT lymphoma cases (*Cp*-positive: P1~P6, *Cp*-negative: N1~N6). The 184 significant methylated CpG sites were selected with the criteria of |delta mean| >0.1 and $p<0.05$. The color scale of the heat map represents densely methylated loci (red) to sparsely methylated loci (green). All cases were clearly clustered into two groups.

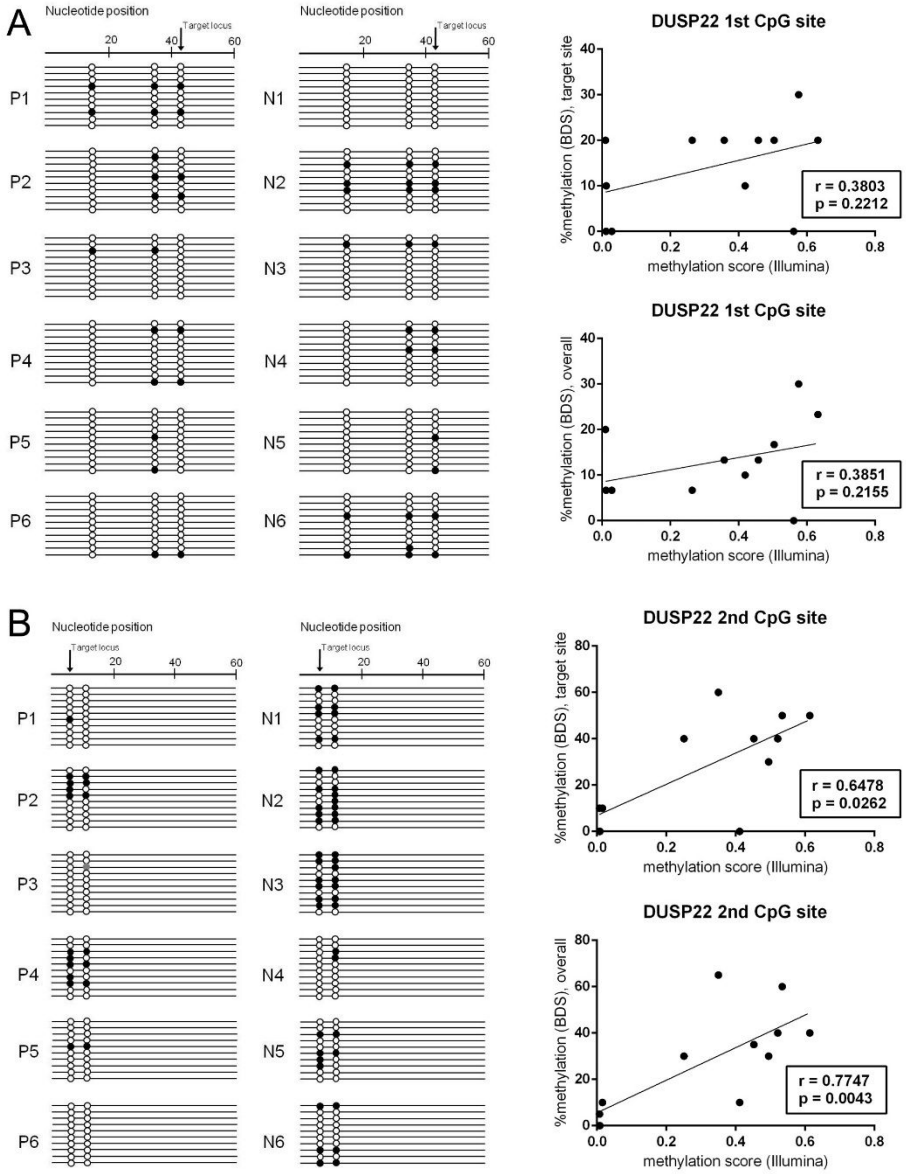

Cp-positive: P1~P6, *Cp*-negative: N1~N6

BDS, bisulfite direct sequencing

Figure 4. Results of direct bisulfite sequencing for 2 differentially methylated CpG sites of *DUSP22* in ocular adnexal MALT lymphoma. A: 1st CpG site, target ID cg15383120, promoter, CpG island. B: 2nd CpG site, target ID cg11235426, nonpromoter, CpG island. Each row represents a bacterial clone with a circle symbolizing a CpG site. Methylated and unmethylated CpG sites are indicated by black and white circles, respectively. Mutated sites are indicated by gray circles. Correlation analysis between Infinium Methylation Chip Assay and bisulfite sequencing revealed that only 2nd CpG site showed significant correlation between two methods.

Table 3. Summary of gene set enrichment analysis with differentially methylated genes according to *Chlamydophila psittaci* infection in ocular adnexal mucosa-associated lymphoid tissue lymphoma

Annotation category by biological processes	Number of involved genes in the category	Number of total genes in the category	*p - value
Immunity and defense	38	2345	8.69E-07
Signal transduction	61	6249	0.00134
Lipid, fatty acid, and steroid metabolism	17	1283	0.01301
Homeostasis	7	301	0.01692
Blood circulation and gas exchange	5	145	0.01756
Neuronal activities	13	900	0.01895
Sensory perception	9	508	0.02227
Coenzyme and prosthetic group metabolism	6	266	0.03492
Annotation category by molecular function			
Receptor	37	2004	5.75E-08
Ion channel	14	543	9.35E-05
Extracellular matrix	10	514	0.00844
Signaling molecule	16	1180	0.01368
Defense and immunity protein	9	493	0.01906
Transfer and carrier protein	8	444	0.03136

*Analyzed by modified one-tail Fisher Exact test

Differential Methylation According to Responsiveness to Doxycycline

With regard to the doxycycline response, the general methylation level was similar between the two groups, showing a bimodal distribution (Figure 5). There were a total of 778 CpG sites differentially methylated at | delta mean | ≥0.06 and p-value<0.05. Several CpG sites corresponded to the same gene, and 697 genes were considered to be differentially methylated. The Doxy-responder samples showed hypermethylation in 442 of the CpG sites (56.8 %, 389 genes) and hypomethylation in 336 of the CpG sites (43.2 %, 308 genes). Figure 6 displays hierarchical clustering data, which clearly distinguished the Doxy-responder samples from the Doxy-nonresponder samples.

The results of the gene set analyses using PANTHER are shown in Table 4. The most significant annotation clusters of enriched gene sets (p < 0.05) were inferred from functional annotation analysis with DMGs according to their methylation statuses. The DMGs were enriched in genes for biologic processes related to signal transduction (p=9.20E-08), followed by developmental processes (p=2.22E-06) and neuronal activity (p=1.01E-05). Regarding molecular function, DMGs were related to receptor (p=2.76E-08), transcription factor (p=0.00015), and extracellular matrix (p=0.00057). To validate the epigenetic control of DMGs for the response to doxycycline, we chose 1 hypomethylated (interleukin-1 receptor-associated kinase 1, *IRAK1*)

and 1 hypermethylated (CXC chemokine ligand 6, *CXCL6*) gene from the signal transduction gene set.

The methylation levels of *IRAK1* and *CXCL6* were examined by pyrosequencing. The results obtained for *IRAK1* and *CXCL6* were in accordance with the results obtained by the Infinium methylation chip assay with the Spearman's rank correlation coefficient (p = 0.0026, Spearman coefficient = 0.8961) and p = 0.0368, Spearman coefficient = 0.7619, respectively) (Figure 7).

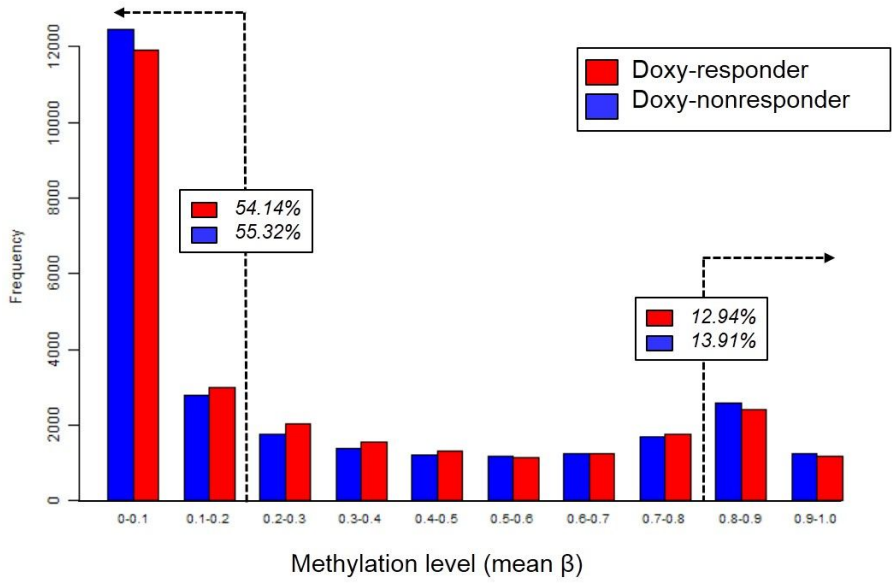

Figure 5. Distribution of the mean β-values of CpG sites in ocular adnexal MALT lymphoma Doxy-responders (n=4) and Doxy-nonresponders (n=4).

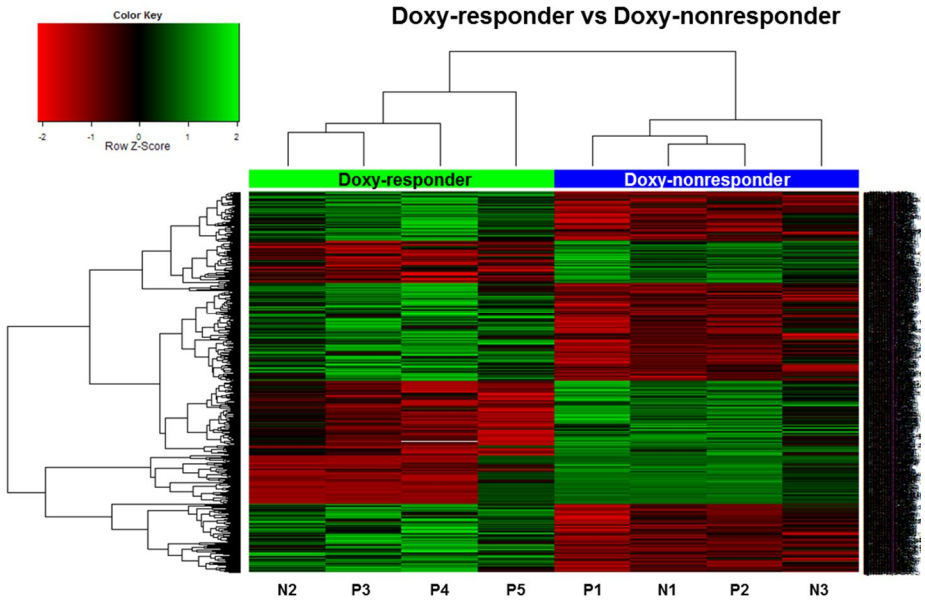

Figure 6. Cluster analysis and heatmap of methylation level between ocular adnexal MALT lymphoma Doxy-responders (n=4) and Doxy-nonresponders (n=4). The methylation levels at the 778 CpG sites were used for hierarchical clustering. All cases were clearly clustered into two groups in this dendrogram.

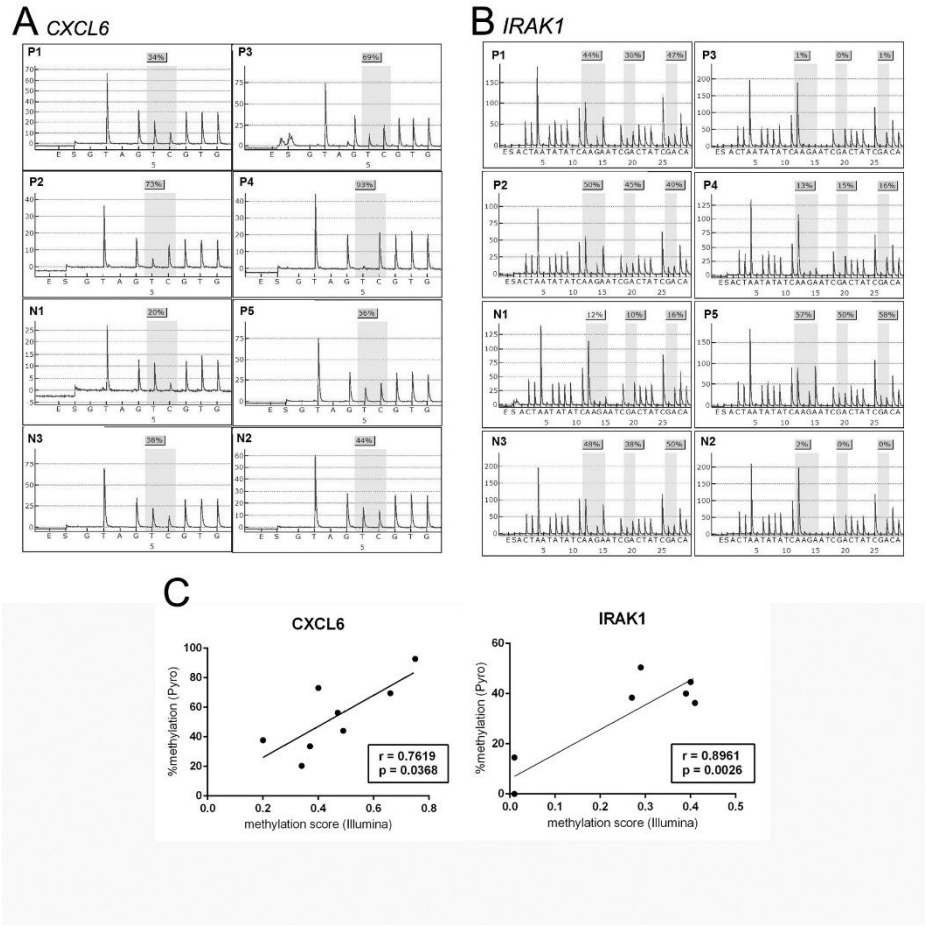

Figure 7. Pyrogram data of (A) *CXCL6* and (B) *IRAK1* in ocular adnexa MALT lymphoma. (C) Correlation analysis between Infinium Methylation Chip Assay and pyrosequencing of *IRAK1* and *CXCL6*.

Table 4. Summary of gene set enrichment analysis with differentially methylated genes according to response to doxycycline in ocular adnexal mucosa-associated lymphoid tissue lymphoma

Annotation category by biological processes	Number of involved genes in the category	Number of total genes in the category	*p - value
Signal transduction	6249	242	9.20E-08
Developmental processes	3771	155	2.22E-06
Neuronal activities	900	51	1.01E-05
Cell adhesion	856	45	0.00018
Immunity and defense	2345	93	0.00113
Oncogenesis	712	34	0.00521
Homeostasis	301	18	0.00727
Apoptosis	825	36	0.01406
Transport	2119	75	0.03827
Annotation category by molecular function			
Receptor	2004	102	2.76E-08
Transcription factor	2709	110	0.00015
Extracellular matrix	514	30	0.00057
Cell adhesion molecule	542	31	0.00062
Ion channel	543	26	0.01481
Defense/immunity protein	493	24	0.01652
Signaling molecule	1180	46	0.02999

*Analyzed by modified one-tail Fisher Exact test

DISCUSSION

Using a genome-wide approach, we compared the methylation state of 27,578 loci of 14,000 genes between *Cp*-positive and *Cp*-negative samples and between samples of responders and non-responders to doxycycline treatment. The cluster analysis showed that all cases could be clearly distinguished based on their *Cp* status using 180 DMGs. The methylation profiles showed a distinct signature according to the response to doxycycline treatment with 778 DMGs.

Over the last decade, *Cp* has been proposed as a possible etiologic agent of ocular adnexal MALT lymphoma (20). The role of *Cp* in the pathogenesis of ocular adnexal MALT lymphoma has not been fully elucidated. *Chlamydophila* species are obligate intracellular bacteria that cause persistent infections. *Cp* infection may trigger a chronic antigenic stimulus that can drive the development of acquired MALT and overt MALT lymphomas (4). In addition to antigenic stimulation, a potential, direct oncogenic role of *Cp* has recently been suggested. Some researchers have reported that these organisms have mitogenic activity, induce oxidative damage, and cause a resistance to apoptosis of the infected cells (21, 22). In this study, there were only 180 DMGs over 14,000 tested genes, and these DMGs were frequently included in gene sets of immunity and defense and signal transduction gene sets; such distinct methylation patterns are likely

attributable to the *Cp* infection itself rather than different oncogenic mechanism.

DUSP22 is one of the atypical *DUSP*s and can activate c-Jun N-terminal kinase (*JNK*) through the activation of the upstream mitogen-activated protein kinase kinase 3 (*MKK3*) and *MKK7* (23). *JNK*s are responsive to stress stimuli and play a role in T cell differentiation and cellular apoptosis, and dysfunctional *JNK* signaling is associated with inflammatory, vascular, neurodegenerative, metabolic, and oncological diseases. There are some studies that have reported the activation of the *JNK* pathway upon *Chlamydophila* infection (24, 25). In the present study, *DUSP22* was hypomethylated in the *Cp*-positive group, which may suggest that the *DUSP22* gene induces gene expression by activating transcription. In addition, *DUSP22* could act as a tumor suppressor gene (26). *DUSP22* is upregulated in B-cell chronic lymphocytic leukemia in patients harboring mutations at the IgVH gene, which regarded as a good prognostic marker (27). *DUSP22* rearrangements have recently been reported in subsets of cutaneous and systemic T-cell lymphomas (28-30). *DUSP22* is also down-regulated in breast cancers, which typically show amplification at the 8p11-12 chromosomal region (31). *DUSP22* is recently suggested as a potential therapeutic target for these disorders (32).

The standard treatment for ocular adnexal MALT lymphoma is low-dose radiotherapy. Although radiotherapy has a very high rate of local control,

ranging from 80 to 100%, potential ocular toxicity and the risk of distant metastasis are its major limitations. Several alternative treatment modalities are available, including chemotherapy, monoclonal anti-CD20 antibody treatment, interferon immunotherapy, and doxycycline antibiotic treatment (15). For gastric MALT lymphoma, antibiotic therapy targeting *Hp* induces lymphoma regression in 60-70 % of stage I_E cases (33). Similarly, *Cp*-eradicating treatment has been suggested for ocular adnexal MALT lymphoma (34). A Korean study with 26 months of follow-up reported a 47% overall response rate to *Cp*-eradicating treatment (14). Doxycycline treatment basically targets *Cp* eradication, but lymphoma regression has been observed in both *Cp*-positive and *Cp*-negative patients, and it is possible that other undiscovered doxycycline-sensitive organisms may be associated with ocular adnexal MALT lymphoma or that doxycycline has an antineoplastic or immunomodulatory effect (35). Thus, we analyzed the methylation profiles according to *Cp* status and the response to doxycycline treatment separately. There were only 9 genes that overlapped between the DMGs determined by the two criteria.

The ontologic analysis of the DMGs according to the response to doxycycline showed that methylation occurred in genes involved in various biological processes and molecular functions. The most distinct ontologic categories were “signal transduction”, “developmental process”, “neuronal activities”, “cell adhesion”, and “immunity and defense”. Some genes

involved in the pathogenesis of ocular adnexal MALT lymphoma deserve our attention and were validated by pyrosequencing. *IRAK1*, which is a serine-threonine kinase, was identified as a key component of the IL-1R signaling pathway and involved in toll-like receptor signaling (36). *IRAK1* has recently been indicated as a gene associated with systemic lupus erythematosus. It also may play a regulatory role in diabetes and atherosclerosis. *CXCL6*, known as granulocyte chemotactic protein 2, is a small cytokine belonging to the chemokine family. Chemokines are known for inducing directional cellular migration during inflammation, and prolonged inflammation is thought to facilitate carcinogenesis by providing a microenvironment that is ideal for tumor cell development and growth (37). *CXCL6* displays angiogenic effects in tumors and is upregulated in gastrointestinal tumors, lung cancer, and osteosarcoma. Interestingly, the angiogenic effect of *CXCL6* correlates with the expression of matrix metalloproteinase (MMP)-9/gelatinase-B, and doxycycline is well-known to have anti-MMP properties. In this study, the Doxy-response group showed *CXCL6* hypomethylation, suggesting elevated *CXCL6* expression. This finding suggests the inhibition of MMP activity is a possible mechanism of action of doxycycline in ocular adnexal MALT lymphoma, but further research will be needed to clarify this point.

We used Illumina's Methylation 27 assay to evaluate DNA methylation profiles of ocular adnexal MALT lymphoma at a genome-wide level. The reproducibility of the Infinium Methylation chip assay was reported

to have a correlation greater than 0.98 between technical replicates (38). In addition, the Infinium Methylation chip assay has been compared to other platforms and has shown reliable results with high correlation rates ranging from 0.8~0.9 (39).

In this study, we used different technical approaches to validate the methylation status of the selected genes. There was a strong correlation between the pyrosequencing and array analysis when we tested *IRAK1* and *CXCL6*. For *DUSP22*, we used bisulfite direct sequencing instead of pyrosequencing to validate two differentially methylated CpG sites because the primer design for pyrosequencing was structurally problematic. For one CpG site (2nd CpG site), the results were highly correlated with those of the array analysis. However, the bisulfite direct sequencing yielded a generally low level of methylation of the other CpG site (1nd CpG site) of *DUSP22* in all samples, which was inconsistent with the methylation chip assay. Although the bisulfite sequencing is one of the most frequently used techniques to measure DNA methylation, the robustness of bisulfite sequencing is dependent on the number of clones examined and is subject to more cloning biases (40). An adequate sample size and larger number of clones will be needed to overcome the variability of the results of bisulfite direct sequencing.

This study had several weaknesses. First, we analyzed 4 Doxy-responder and 4 Doxy-nonresponders regardless of their *Cp* status because of the small sample size. Although several studies have reported that the

response rate to doxycycline treatment and *Cp* status were not associated, samples with uniform characteristics will help to verify the mechanism of doxycycline treatment in ocular adnexal MALT lymphoma cases.[14, 34] Second, we analyzed only the DNA methylation status, and further experiments are required explore the relationship between the methylation status and mRNA expression with a much greater number of samples. Many epigenetic alterations in cancer can be passenger events that are not pathogenic and, thus, should be supported by gene expression analysis. In future studies, the correlation between methylation status and gene expression should be addressed.

CONCLUSIONS

This study is the first report on methylation profiles based on a genome-wide methylation in ocular adnexal MALT lymphoma tissues. The results demonstrated that a number of genes were methylated differentially with regards to *Cp* infection status and the response to doxycycline treatment. Among the candidate genes, the methylation of *DUSP22* was likely attributable to *Cp* infection. The methylation status of *IRAK1* and *CXCL6* were quite different between the Doxy-responders and Doxy-nonresponders, suggesting the possible clinical application of therapies targeting those genes. Further, large-scaled studies are warranted to confirm our results.

REFERENCES

1. Stefanovic A, Lossos IS. Extranodal marginal zone lymphoma of the ocular adnexa. Blood. 2009 Jul 16; 114(3):501-510.

2. Coupland SE, Krause L, Delecluse HJ, et al. Lymphoproliferative lesions of the ocular adnexa. Analysis of 112 cases. Ophthalmology. 1998 Aug; 105(8):1430-1441.

3. Moslehi R, Devesa SS, Schairer C, Fraumeni JF, Jr. Rapidly increasing incidence of ocular non-hodgkin lymphoma. J Natl Cancer Inst. 2006 Jul 5; 98(13):936-939.

4. Ferreri AJ, Dolcetti R, Du MQ, et al. Ocular adnexal MALT lymphoma: an intriguing model for antigen-driven lymphomagenesis and microbial-targeted therapy. Ann Oncol. 2008 May; 19(5):835-846.

5. Oh DE, Kim YD. Lymphoproliferative diseases of the ocular adnexa in Korea. Arch Ophthalmol. 2007 Dec; 125(12):1668-1673.

6. Yoon JS, Ma KT, Kim SJ, Kook K, Lee SY. Prognosis for patients in a Korean population with ocular adnexal lymphoproliferative lesions. Ophthal Plast Reconstr Surg. 2007 Mar-Apr; 23(2):94-99.

7. Sullivan TJ, Whitehead K, Williamson R, et al. Lymphoproliferative disease of the ocular adnexa: a clinical and pathologic study with statistical analysis of 69 patients. Ophthal Plast Reconstr Surg. 2005 May; 21(3):177-188.

8. Suarez F, Lortholary O, Hermine O, Lecuit M. Infection-associated

lymphomas derived from marginal zone B cells: a model of antigen-driven lymphoproliferation. Blood. 2006 Apr; 107(8):3034-3044.

9. Ferreri AJ, Guidoboni M, Ponzoni M, et al. Evidence for an association between Chlamydia psittaci and ocular adnexal lymphomas. J Natl Cancer Inst. 2004 Apr; 96(8):586-594.

10. Carugi A, Onnis A, Antonicelli G, et al. Geographic variation and environmental conditions as cofactors in Chlamydia psittaci association with ocular adnexal lymphomas: a comparison between Italian and African samples. Hematol Oncol. 2010 Mar; 28(1):20-26.

11. Chanudet E, Zhou Y, Bacon CM, et al. Chlamydia psittaci is variably associated with ocular adnexal MALT lymphoma in different geographical regions. J Pathol. 2006 Jul; 209(3):344-351.

12. Yoo C, Ryu MH, Huh J, et al. Chlamydia psittaci infection and clinicopathologic analysis of ocular adnexal lymphomas in Korea. Am J Hematol. 2007 Sep; 82(9):821-823.

13. Choung HK, Kim YA, Lee MJ, Kim N, Khwarg SI. Multigene methylation analysis of ocular adnexal MALT lymphoma and their relationship to Chlamydophila psittaci infection and clinical characteristics in South Korea. Invest Ophthalmol Vis Sci. 2012 Apr; 53(4):1928-1935.

14. Kim TM, Kim KH, Lee MJ, et al. First-line therapy with doxycycline in ocular adnexal mucosa-associated lymphoid tissue lymphoma: a

retrospective analysis of clinical predictors. Cancer Sci. 2010 May; 101(5):1199-1203.

15. McKelvie PA. Ocular adnexal lymphomas: a review. Adv Anat Pathol. 2010 Jul; 17(4):251-261.

16. Kondo T, Oka T, Sato H, et al. Accumulation of aberrant CpG hypermethylation by Helicobacter pylori infection promotes development and progression of gastric MALT lymphoma. Int J Oncol. 2009 Sep; 35(3):547-557.

17. Kaneko Y SS, Hironaka M, et al. Distinct methylated profiles in Helicobacter pylori dependent and independent gastric MALT lymphomas. Gut. 2003; 52(5):641-646.

18. Coupland SE, White VA, Rootman J, Damato B, Finger PT. A TNM-based clinical staging system of ocular adnexal lymphomas. Arch Pathol Lab Med. 2009 Aug; 133(8):1262-1267.

19. Cheson BD, Horning SJ, Coiffier B, et al. Report of an international workshop to standardize response criteria for non-Hodgkin's lymphomas. NCI Sponsored International Working Group. J Clin Oncol. 1999 Apr; 17(4):1244.

20. Collina F, De Chiara A, De Renzo A, De Rosa G, Botti G, Franco R. Chlamydia psittaci in ocular adnexa MALT lymphoma: a possible role in lymphomagenesis and a different geographical distribution. Infect Agent Cancer. 2012 Apr; 7:8.

21. Sharma M, Rudel T. Apoptosis resistance in Chlamydia-infected cells: a fate worse than death? FEMS Immunol Med Microbiol. 2009 Mar; 55(2):154-161.

22. Kun D, Xiang-Lin C, Ming Z, Qi L. Chlamydia inhibit host cell apoptosis by inducing Bag-1 via the MAPK/ERK survival pathway. Apoptosis. 2013 Sep; 18(9):1083-1092.

23. Shen Y, Luche R, Wei B, Gordon ML, Diltz CD, Tonks NK. Activation of the Jnk signaling pathway by a dual-specificity phosphatase, JSP-1. Proc Natl Acad Sci U S A. 2001 Nov; 98(24):13613-13618.

24. Rodriguez N, Lang R, Wantia N, et al. Induction of iNOS by Chlamydophila pneumoniae requires MyD88-dependent activation of JNK. J Leukoc Biol. 2008 Dec; 84(6):1585-1593.

25. Krull M, Kramp J, Petrov T, et al. Differences in cell activation by Chlamydophila pneumoniae and Chlamydia trachomatis infection in human endothelial cells. Infect Immun. 2004 Nov; 72(11):6615-6621.

26. Nunes-Xavier C, Roma-Mateo C, Rios P, et al. Dual-specificity MAP kinase phosphatases as targets of cancer treatment. Anticancer Agents Med Chem. 2011 Jan; 11(1):109-132.

27. Jantus Lewintre E, Reinoso Martin C, Garcia Ballesteros C, et al. BCL6: somatic mutations and expression in early-stage chronic lymphocytic leukemia. Leuk Lymphoma. 2009 May; 50(5):773-780.

28. Bisig B, Gaulard P, de Leval L. New biomarkers in T-cell lymphomas. Best Pract Res Clin Haematol. 2012 Mar; 25(1):13-28.

29. Karai LJ, Kadin ME, Hsi ED, et al. Chromosomal rearrangements of 6p25.3 define a new subtype of lymphomatoid papulosis. Am J Surg Pathol. 2013 Aug; 37(8):1173-1181.

30. Sciallis AP, Law ME, Inwards DJ, et al. Mucosal CD30-positive T-cell lymphoproliferations of the head and neck show a clinicopathologic spectrum similar to cutaneous CD30-positive T-cell lymphoproliferative disorders. Mod Pathol. 2012 Jul; 25(7):983-992.

31. Bernard-Pierrot I, Gruel N, Stransky N, et al. Characterization of the recurrent 8p11-12 amplicon identifies PPAPDC1B, a phosphatase protein, as a new therapeutic target in breast cancer. Cancer Res. 2008 Sep; 68(17):7165-7175.

32. Patterson KI, Brummer T, O'Brien PM, Daly RJ. Dual-specificity phosphatases: critical regulators with diverse cellular targets. Biochem J. 2009 Mar; 418(3):475-489.

33. Isaacson PG, Du MQ. MALT lymphoma: from morphology to molecules. Nat Rev Cancer. 2004 Aug; 4(8):644-653.

34. Ferreri AJ, Ponzoni M, Guidoboni M, et al. Bacteria-eradicating therapy with doxycycline in ocular adnexal MALT lymphoma: a multicenter prospective trial. J Natl Cancer Inst. 2006 Oct; 98(19):1375-1382.

35. Ferreri AJ. Activity of clarithromycin in mucosa-associated lymphoid tissue-type lymphomas: antiproliferative drug or simple antibiotic? Chest. 2011 Mar; 139(3):724-725; author reply 725-726.

36. Gottipati S, Rao NL, Fung-Leung WP. IRAK1: a critical signaling mediator of innate immunity. Cell Signal. 2008 Feb; 20(2):269-276.

37. Vandercappellen J, Van Damme J, Struyf S. The role of CXC chemokines and their receptors in cancer. Cancer Lett. 2008 Aug; 267(2):226-244.

38. Bibikova M, Le J, Barnes B, et al. Genome-wide DNA methylation profiling using Infinium(R) assay. Epigenomics. 2009 Oct; 1(1):177-200.

39. Bock C, Tomazou EM, Brinkman AB, et al. Quantitative comparison of genome-wide DNA methylation mapping technologies. Nat Biotechnol. 2010 Oct; 28(10):1106-1114.

40. Reed K, Poulin ML, Yan L, Parissenti AM. Comparison of bisulfite sequencing PCR with pyrosequencing for measuring differences in DNA methylation. Anal Biochem. 2010 Feb 1; 397(1):96-106.

국문 초록

배경 및 목표: 안구부속조직 림프종은 안구부속조직에서 발생하는 악성 종양 중 그 빈도가 가장 높으며, 그 중 점막기원 림프종이 가장 흔한 조직학적 아형으로 알려져 있다. 최근 *Chlamydophila psittaci* (*Cp*)가 안구부속조직 점막기원 림프종의 발생에 중요한 역할을 하는 원인 인자로 전세계적으로 많은 연구가 이루어져 왔으며, 특히 한국에서는 안구부속조직 점막기원 림프종 조직에서의 *Cp* DNA 양성율이 높게 보고되어 왔다. 또한 이를 바탕으로 *Cp*를 표적으로 한 독시사이클린 항생제 치료가 시도되고 있다. 한편, 안구부속조직 점막기원 림프종의 발생과 연관된 유전 이상 중, 몇몇 종양억제유전자의 과메틸화에 관련된 보고들이 있어 왔으나, 유전자 전체 수준에서의 메틸화의 양상에 대해서는 알려져 있는 바가 없다. 따라서 본 연구에서는 한국인의 안구부속조직 점막기원 림프종에서 *Cp* 감염 여부과 독시사이클린 치료의 반응에 따라 전체 유전자 수준에서의 메틸화 양상을 비교 분석해 보고자 하였다.

방법: 12명의 안구부속조직 점막기원 림프종 환자를 대상으로 하여, 신선 조직에서 DNA를 추출하였다. *Cp* DNA 검출 유무에 따라 *Cp* 양성군 (6명)과 *Cp* 음성군 (6명)으로 나누었다. 이 중 독시사이클린 경구 치료를 초기 치료로 시행받고 6개월 이상 경과를 관찰한 8명을 치료 반응 정도에 따라 치료 반응군 (4명)과 치료 비반응군 (4명)으로 나누었다. Infinium Methylation chip

assay를 이용하여 14,000개의 유전자에 분포된 27,578 개의 CpG 자리의 메틸화 정도(β)를 측정하여 *Cp* 양성군과 *Cp* 음성군, 치료 반응군과 치료 비반응군 사이에 비교 분석하였다. β평균의 차이가 < -0.06 혹은 > 0.06 이면서 $p < 0.05$ 인 유전자를 DMG (differentially methylated gene, 유의하게 메틸화의 정도가 차이나는 유전자)로 정의하고, 가장 메틸화의 차이가 큰 몇 몇 DMG들에 대해 bisulphite direct sequencing 혹은 pyrosequencing의 방법을 이용하여 검증을 시행하였다.

결과: Infinium Methylation chip assay를 이용하여 전체 유전자의 메틸화 정도를 분석하였을 때, *Cp* 음성군을 기준으로 *Cp* 양성군에서 과메틸화를 보이는 유전자가 74개, 저메틸화를 보이는 유전자가 106개로, 두 군 사이에 180개의 DMG가 발견되었다. 그 중, 2개의 유의한 메틸화 차이를 보이는 CpG 자리를 가진 *DUSP22* 유전자에 대한 검증을 bisulphite direct sequencing을 이용하여 시행하였고, 하나의 CpG 자리는 Infinium Methylation chip assay와 유의한 상관 관계를 보이지 않았으나 (Spearman coefficient=0.3803, p=0.2212), 다른 하나의 CpG 자리는 유의한 상관 관계를 나타내었다 (Spearman coefficient = 0.6478, p = 0.0262). 독시사이클린 치료 반응군과 치료 비반응군 사이에서는 전체 778개의 DMG가 발견되었으며, 치료 비반응군에 비해 치료 반응군에서 과메틸화 되어있는 유전자가 389개, 저메틸화 되어있는 유전자가 336개였다. 이 중 *IRAK1* 유전자와 *CXCL6* 유전자에

대해 pyrosequencing을 이용하여 검증을 시행하였으며, Infinium Methylation chip study와 유의한 상관관계를 나타내었다 (*IRAK1*; Spearman coefficient = 0.8961, p = 0.0026, *CXCL6*; Spearman coefficient = 0.7619, p = 0.0368)

결론: 본 연구를 통해 안구부속조직 점막관련 림프종에서 *Cp* 감염 여부과 독시사이클린 반응 여부에 따라 전체 유전자 수준에서의 메틸화 양상이 상이하게 나타남을 확인할 수 있었다. 또한 *DUSP22* 유전자의 메틸화 상태가 Cp 감염과 관련이 있으며, *IRAK1*과 *CXCL6* 유전자는 독시사이클린 반응 여부에 따라 유의한 메틸화의 차이를 나타내었다. 본 연구결과는 안구부속조직 점막관련 림프종의 병인 규명 및 치료 결과 예측에 기여할 수 있을 것으로 예상된다.

주요어: 안구부속조직, 점막기원 림프종, 유전자의 메틸화,
Chlamydophila psittaci, 독시사이클린, *DUSP22*, *IRAK1*, *CXCL6*
학 번: 2008-31013